RESEARCH ARTICLE



Dynamic Simulation of a Hybrid Energy System for Powering a Water Treatment Facility in McCallum, Newfoundland and Labrador

Fatemeh Kafrashi* and Tariq Iqbal

ABSTRACT

Clean water, a basic human need, is in short supply in McCallum, Newfoundland and Labrador, primarily due to lead contamination, forcing residents to rely on collected rainwater. Reverse Osmosis (RO) has been identified as the most suitable desalination method because of its lower energy requirements and high effectiveness in treating lead-contaminated water. Powering the RO system with renewable energy sources (RES) offers a promising solution for this remote, off-grid area, currently powered by a diesel generator. The proposed hybrid energy system (HES) provides not only the most economically optimal configuration but also greater reliability. The system consists of a 3.6 kW solar array, a 2-kW wind turbine, a 3-kW DC diesel generator, and a 680 Ah 48 V battery bank to supply the single-phase water treatment system, which includes a 0.3 kW resistive load, lighting, and two asynchronous machines rated at 0.5 hp and 0.75 hp, respectively. A dynamic simulation of the proposed system, based on calculation done in Kafrashi and Iqbal [1], is presented in this paper. All system components are modeled in MATLAB/Simulink. Simulation results show expected dynamics in the system. Results indicate proper system operation with reasonable within-range system voltage and current during normal operation.

Keywords: Hybrid Energy System (HES), Photovoltaic (PV), Reverse Osmosis (RO), Wind Turbine (WT).

Submitted: November 13, 2024

Published: December 31, 2024

6 10.24018lejenergy.2024.4.4.157

Department of Electrical and Computer Engineering, Memorial University of Newfoundland, Canada.

*Corresponding Author: e-mail: fkafrashi@mun.ca

1. Introduction

The lack of freshwater is becoming a major concern in many regions due to climate change and water pollution. Desalination offers a sustainable solution to meet water demand in areas where untreated water sources are available. Two main desalination methods that are economically reliable for producing freshwater in areas experiencing water shortages are Thermal-based (MSF, MED, VC) and Membrane-based (RO, ED). Among these desalination technologies, RO (Reverse Osmosis) is the most effective because it is independent of thermal energy, which lowers its power consumption. The power demand for this method ranges from 2 kWh to 5 kWh per m³ of water, depending on the source of water, whether brackish or seawater [2]. A promising alternative to traditional, fossil fuel-powered RO desalination systems is a hybrid approach that integrates renewable energy sources (RES) like wind or solar energy with RO desalination. By directly coupling energy generation from RES to RO systems, the costs associated with transmission and distribution (COE) can be avoided, leading to a significant reduction in the overall COE of desalination systems [3]. A backup energy system is typically paired with both photovoltaic (PV) systems and wind energy systems (WES) to ensure a continuous power supply despite the inherent intermittency of renewable energy sources. Diesel generators (DG) and battery energy storage (BES) are the primary backup solutions used to address the variability in power supply from wind and solar due to weather changes. Diesel generators need fuel and regular maintenance, and their emissions contribute to pollution, whereas batteries, though costly and having a shorter lifespan, provide a cleaner alternative [4].

Many studies have explored various configurations of HES to power RO systems, particularly in arid and remote areas. For instance, Cervantes-Rendón *et al*. [5] examined an efficient PV system in Mexico, where solar energy is abundant, as a sustainable solution to power a low-pressure RO system. This system supplied fresh water

for a family of three on an annual basis while minimizing environmental impact and reducing costs. Similarly, Apolinário and Castro [6] presented a case study from Portugal demonstrated that integrating PV with RO systems reduced desalination costs by 33%, making this method economically viable compared to grid-powered alternatives.

In the United Arab Emirates, Loutatidou et al. [7] proposed a wind-driven RO system as part of the Liwa Aquifer Storage and Recovery (ASR) project. This design allowed desalination output to fluctuate based on wind availability, eliminating the need for costly energy storage. However, this flexibility introduced challenges such as increased capital costs due to the necessity of oversizing the plant to ensure continuous operation during periods of wind variability.

A study by Eltamaly et al. [8] in Saudi Arabia optimized the integration of wind energy and solar energy with RO systems, balancing the intermittency of wind by hybrid configurations with energy storage systems. The studied system generated 2440 kW of power, sufficient to produce 1000 m³ of water per day.

This paper presents a dynamic simulation of a novel offgrid HES that combines wind and PV power to electrify a water treatment facility in McCallum, Newfoundland and Labrador. Designed to deliver clean, reliable energy for freshwater production, the system leverages local wind speeds and solar irradiance, achieving a cost-effective levelized electricity cost of 0.397 CAD per kWh [1]. This makes it an attractive alternative for remote communities reliant on diesel generators with subsidized rates to match grid-connected electricity costs, which is 14 cents per kWh. In contrast, this renewable-based HES provides a more sustainable and economical solution, reducing reliance on expensive, polluting diesel power. The design includes a small diesel generator and battery backup to maintain consistent operation during low renewable output, addressing key gaps in stability, efficiency, and cost-effectiveness for isolated areas where grid electricity is prohibitively expensive. Comprehensive long-term data on renewable resources informed the system's design and implementation. Section 2 provides details of the dynamic modeling of the components of the studied HES. Section 3 presents simulation results, and finally, Section 4 discusses the conclusions of the study.

2. STUDIED HES

The proposed configuration of the HES under study includes a photovoltaic system integrated with a wind energy system, a battery system, a small DC diesel generator, an inverter, and a step-up transformer, as illustrated in the configuration of the total system in MATLAB Simulink in Fig. 1. A detailed design and system sizing can be found in Kafrashi and Iqbal [1].

Specifications of the hybrid energy system are listed in Table I, detailing the capacity of each. More details may be found in Kafrashi and Iqbal [1]. It should be noted that the system is off-grid in a remote community, and it is DCcoupled hybrid power system with 48 V DC bus voltage.

2.1. Solar Power System

The solar conversion system (SCS) consists of a PV system and a pulse-width modulation (PWM) system created by the P&O MPPT method for switching control of a buck converter with the MPPT method. The power extracted from this system can be determined using the specific site resource conditions and the PV array specifications provided by the manufacturer. The amount of generated power (P_{PV}) can be calculated using (1):

$$P_{PV} = G_I \times A_M \times \in_P \tag{1}$$

where G_I denotes the average solar global horizontal irradiance (kW/m²), A_M is the surface area of the PV array, \in_P is the efficiency of array [9]. At the selected site, G_I is 3.17 (kW/m^2) [10], while A_M and \in_P are 1.456 m² and 15.17%, respectively [11]. Fig. 2 shows the simulated solar system in Simulink/MATLAB.

2.1.1. PV System

Based on the calculation done in [1], two 72-cell modules are connected in series and six strings in parallel. P_V curve related to the total array at 25°C is shown in Fig. 3 and module specification is listed in Table II.

2.1.2. Buck Converter

The voltage is stepped down from 73 V to 48 V using a buck converter suitable for the DC bus voltage. In continuous conduction mode (current through the inductor never falls to zero), the theoretical transfer function of the buck converter is:

$$\frac{V_{out}}{V_{in}} = D \tag{2}$$

where *D* is the duty cycle.

L and C are respectively equal to 0.0022 H and 1.9553e-05 F in buck converter using (2) to (7):

$$I_{outmax} = \frac{P}{V_{out}} \tag{3}$$

$$delI_L = 0.01 \times I_{outmax} \tag{4}$$

$$delV_{out} = 0.01 \times V_{out} \tag{5}$$

$$L = (V_{out} \times (V_{in} - V_{out}))/(delI_L \times f_s \times V_{in})$$
 (6)

$$C = (delI_L/(8 \times f_s \times delV_{out})$$
 (7)

$$I_{outmax} = \frac{P}{V_{out}} \tag{8}$$

where P is the power of the PV array, V_{in} and V_{out} are the typical input voltage and desired output voltage, respectively. Furthermore, f_s is the minimum switching frequency of the converter $delI_L$ and $delV_{out}$ represent inductor ripple current and output voltage ripple.

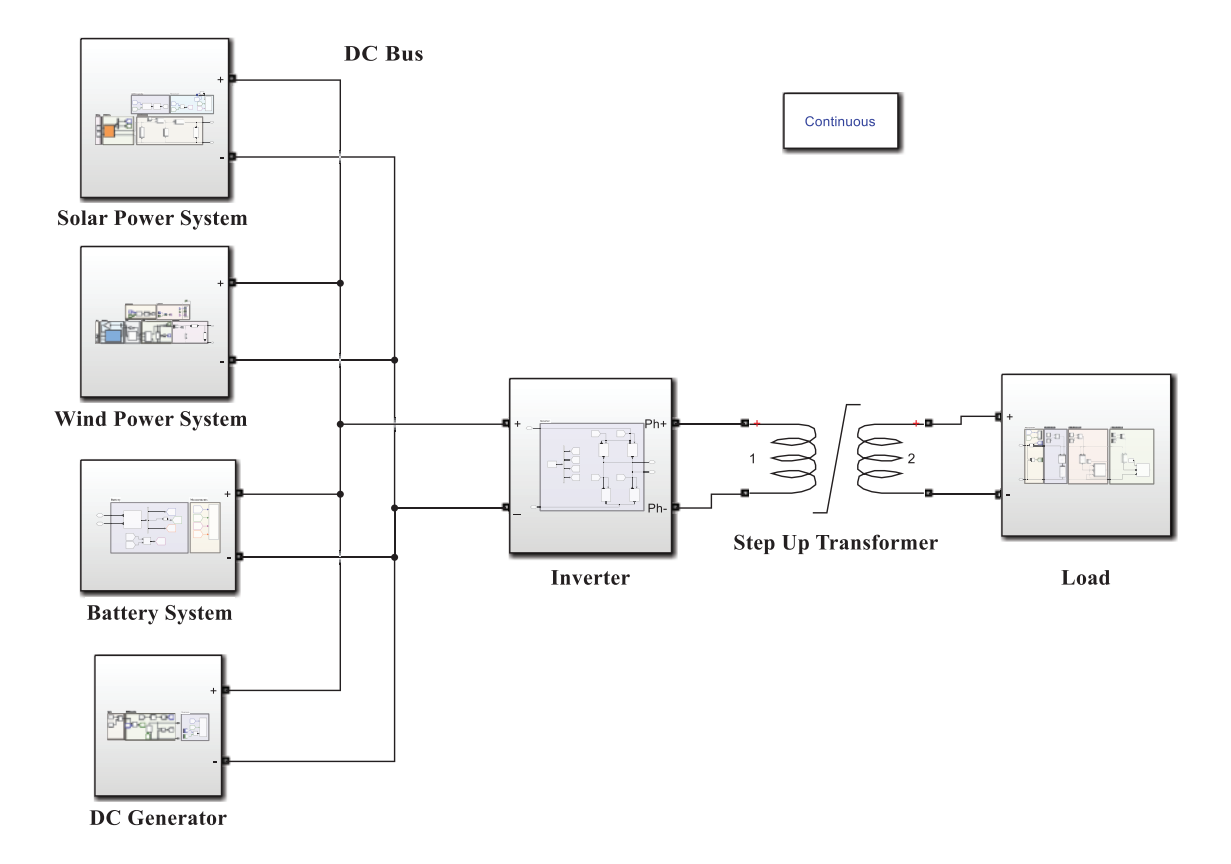


Fig. 1. Hybrid energy system configuration.

TABLE I: Hybrid Energy System Details

Component	Specification	Capacity
PV array	300 Wp Panasonic	3.6 kW
Wind turbine	HAWT	2 kW
Diesel generator	DC	3 kW
Batteries	Lead acid	12 v 680 Ah
Load 1 (Resistive)	Lighting	0.3 kW
Load 2 (Inductive)	Asynchronous machine 1	0.38 kW (0.5 hp)
Load 3 (Inductive)	Asynchronous machine 2	0.56 kW (0.75 hp)

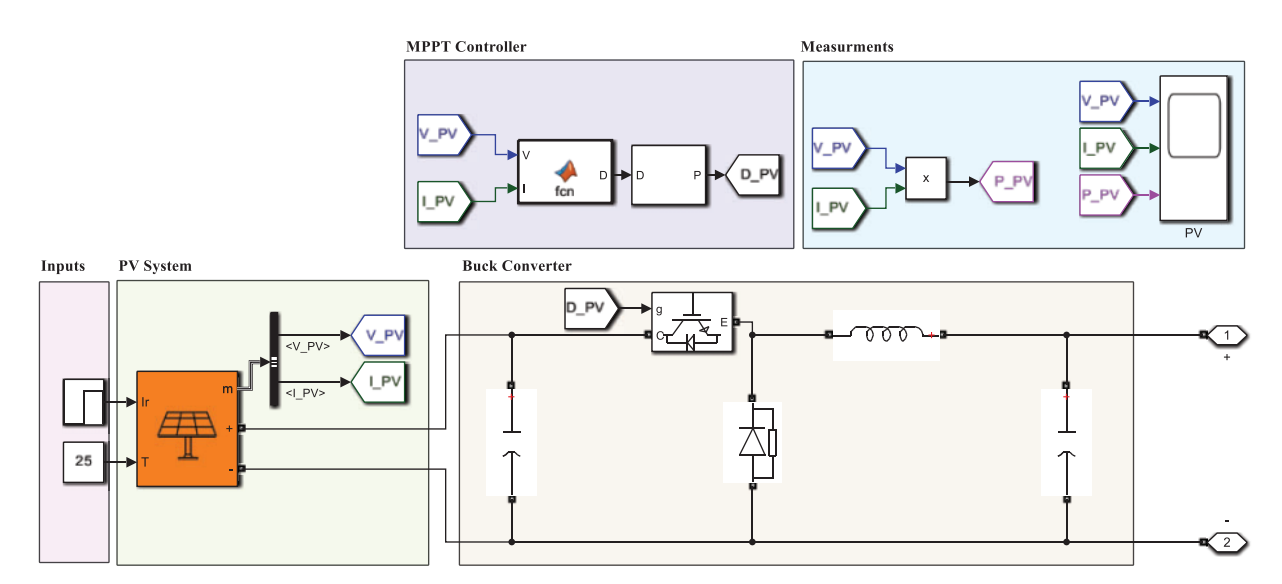


Fig. 2. Solar power system configuration.

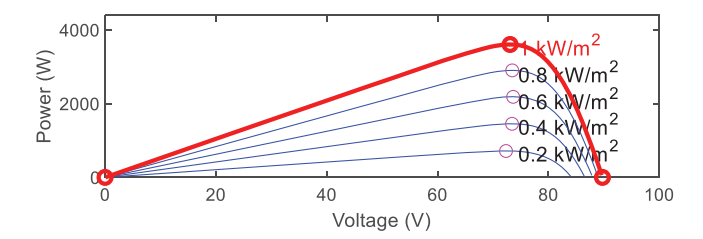


Fig. 3. The array P-V curve.

TABLE II: EACH PV MODULE SPECIFICATIONS [11]

Parameter	Value
Maximum power (W)	300.3588
Open circuit voltage V_{OC} (V)	44.87
Short-circuit current I_{SC} (A)	8.73
Voltage at maximum power point V_{mp} (V)	36.54
Current at maximum power point I_{mp} (A)	8.22
Temperature coefficient of V_{OC} (%/°C)	-0.312

2.1.3. MPPT Method

PV systems should operate at their maximum potential regardless of varying environmental and load conditions. To extract the highest possible power from a PV panel the maximum power point tracking (MPPT) method is used. Typically, a DC-DC power converter works alongside the PV array, with its duty cycle determined by the MPPT system [12]. Here, among all MPPT methods, Perturb and Observe (P&O) is used. The method checks the current or voltage at the PV array's terminals regularly and compares it with the power output. If adjusting the voltage results in increased power (meaning the change in power, ΔPPV , is positive), the adjustment continues in the same direction. However, if the power decreases, the adjustment is reversed. This process is repeated until the maximum power is reached or the change in power becomes zero $(\Delta PPV = 0)$ [13].

2.2. Wind Power System

The wind energy control system (WECS) is considered a direct-drive setup. It consists of a wind turbine, a multipole permanent magnet synchronous generator (PMSG), and a pulse-width modulation (PWM) system created by P&O MPPT method for switching control of a buck converter with MPPT method for charging the battery bank. The power that can be extracted by the electric generator in a wind turbine system P_{WT} can be expressed by (9):

$$P_{WT} = \frac{1}{2}\rho \times A \times V^3 \tag{9}$$

where ρ represents the air density (kg/m³), A is the rotorswept area by the blades, V is the wind speed, and C_P is the power coefficient. At the selected site average yearly V 5.9 m/s [14] is Fig. 4 illustrates the simulated wind power system in Simulink/MATLAB.

2.2.1. Wind Turbine

A horizontal axis wind turbine (HAWT), upwind, with nominal mechanical output power of 2 kW in 12 m/s base wind speed is selected in this model. The turbine power characteristics are shown in Fig. 5.

2.2.2. PMSG

To convert acquired mechanical power to electrical power, a three-phase permanent magnet synchronous Generator (PMSG) with sinusoidal back EMF waveform offering low noise and consistently impressive efficiency is used. The rotor's excitation field is produced by electromagnets and the generator doesn't need power to energize its windings. While the wind turbine rotates the rotor, three-phase power is generated in the stator windings. The PMSG wind turbine model is favored for its straightforward design. By incorporating permanent magnets, it eliminates the need for commutators, slip rings, and brushes, significantly boosting system reliability [15]. The rotors use permanent magnets rather than field windings, resulting in a lower pole count. This reduction in poles decreases reactive power, enhancing the quality of the output [16]. In these variable speed generators, the rotor speed adjusts in direct relation to the increasing wind speed, maintaining a consistent tip-speed ratio (TSR) and performance throughout the operation. This consistency ensures that the turbine operates at peak efficiency across a broad spectrum of wind speeds [17]. The stator windings of PMSG are connected in wye to an internal neutral point, and the rotor is round. Table III shows related specifications of selected PMSG [18].

The selected wind turbine is direct-driven and has no gearbox, meaning the rotor and generator rotate at the same speed. This gearless design reduces weight, losses, costs, and maintenance, making it a more efficient and robust solution.

Wind turbines can be categorized into two main types based on pitch angle: variable pitch and fixed pitch. In variable-pitch wind turbines, the rotor blades can rotate along their longitudinal axis, allowing the pitch angle to change. Conversely, in fixed-pitch wind turbines, the blades are securely attached to the hub, keeping the pitch angle constant at zero [19]. In other words, Pitch angle adjustment of the blades limits the output power by varying the aerodynamic forces acting on the blades at higher wind speeds. In this case, the pitch angle is zero, and no pitch angle control is adopted to avoid complexity and cost. The selected wind turbine has no pitch control.

2.2.3. Rectifier

Due to the varying rotor speed and the resulting fluctuations in the frequency of the generated electricity, power converters are necessary [17]. Maintaining a unity power factor and ensuring a continuous load current. Permanent magnets will energize the rotor windings, and the stator windings will be linked directly to the DC bus Voltage through a rectifier [15]. Therefore, a 3-arm universal bridge, rectifier, is used at the generator output to convert AC voltage to DC rectified voltage, which can be calculated using (10):

$$V_r = \frac{3\sqrt{2}}{\pi} V_{LL} \tag{10}$$

where V_{LL} is line-to-line input voltage of the rectifier.

2.2.4. Buck Converter

To step down the rectifier voltage to an output voltage of 48 V, considering the wind turbine power and a switching

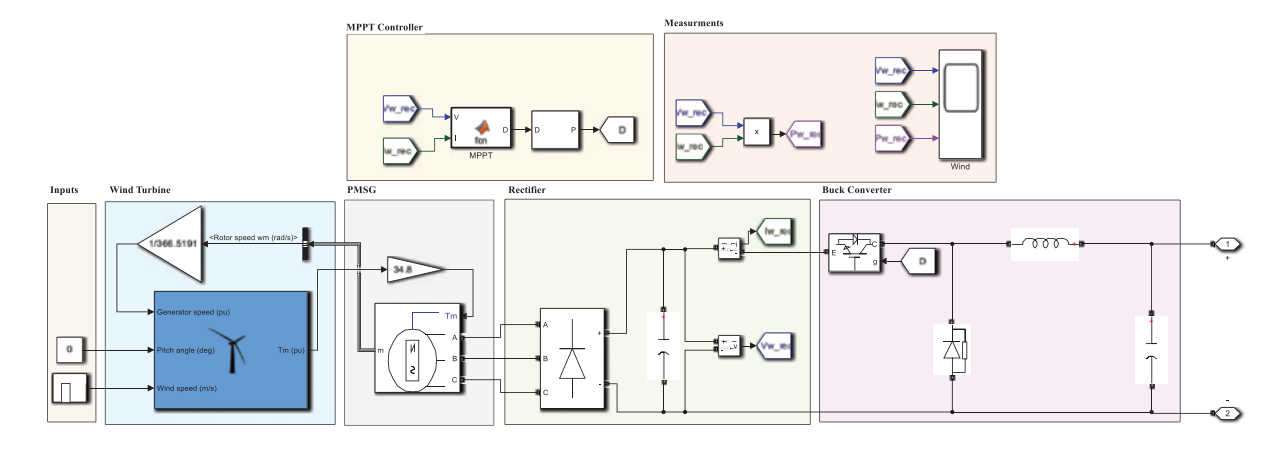


Fig. 4. Wind power system configuration.

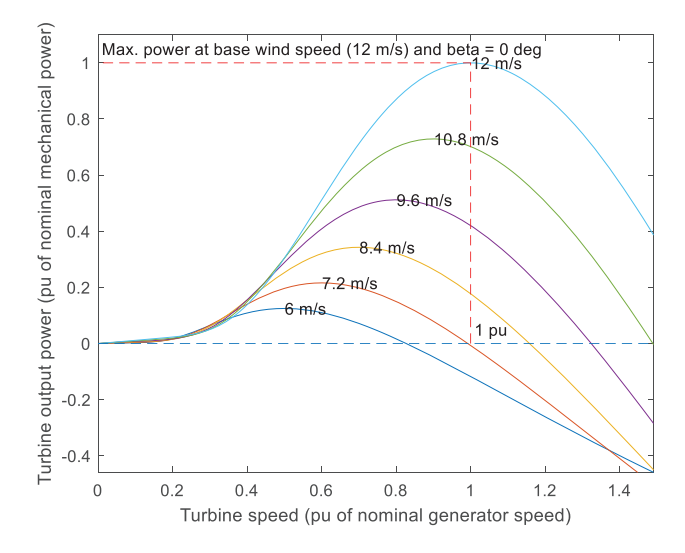


Fig. 5. Turbine power characteristics with zero pitch angle.

frequency of 1000 Hz, a buck converter is designed. The converter includes an IGBT, diode, inductor, and capacitor, with the IGBT controlled by a duty cycle generated by MPPT. Based on (2)–(8), L and C are 6.7765e-04 H and 1.0851e-05 F, respectively.

2.2.5. MPPT Method

The MPPT algorithm is used to harness the maximum available power from the WECS in varying ambient

TABLE III: PMSG SPECIFICATION

IIIDEE III. I NOO DI EGNICINION				
Parameter	Value			
Rated power (kW)	2			
Rated speed (RPM)	1800			
Rated voltage (V)	48 VDC			
Rated current (A)	0.10			
Torque constant Kt (Nm/Arms)	0.09			
No. of phases	Three phase			
Rotor inertia (kg/m ²)	0.002029			
Power factor	≈1			
Efficiency	Designed for 93%			
Winding method	Star/Y			
Insulation resistance	>500 MΩ at 500 Vdc			

conditions. Here, the P&O approach, utilizing a straightforward algorithm, enables us to locate the maximum power point without the need for a wind speed sensor or prior knowledge of the aerodynamic characteristics curve. In the P&O method, the rotor speed is adjusted in small increments, and the resulting changes in output power are measured. For a PMSG, the output current is directly related to the rotor torque, and the voltage is directly related to the rotor speed. Therefore, changing the generator's output voltage will alter the rotor speed accordingly. This voltage variation can be achieved by adjusting the duty cycle of the PWM signal in the buck converter. By monitoring the resulting power, the duty cycle is either increased or decreased in the next cycle. If increasing the duty cycle results in a higher power, the perturbation direction remains the same as the previous cycle. Conversely, if increasing the duty cycle decreases the power, the perturbation direction is reversed from the previous cycle [20].

2.3. Small DC Diesel Generator

For more backup in case of shortage of wind and irradiance, a constant DC-controlled current source is used to provide power, as seen in Fig. 6. The controlled current source is used due to its precise control and flexibility; additionally, it can quickly adjust to varying load conditions, enhancing system efficiency and stability.

2.4. Battery

Battery storage is created by integrating cells with positive and negative electrodes in an electrolyte, using the electrochemical features of an oxidant-reductant pair, where chemical energy is converted into electrical energy [21]. The electrical model related to lead acid battery storage is considered based on an equivalent circuit consisting of a voltage source, an internal resistor, and a capacitor, as shown in Fig. 7 [22].

As a result, the mathematical model will be formulated as (11):

$$U_{bat} = E_0 - \left(K \cdot \frac{\int I_b dt}{Q_0}\right) - R_b \cdot I_b \tag{11}$$

where E_0 is the initial voltage in the charged battery (V), K is constant specific to the battery, R_b is the internal

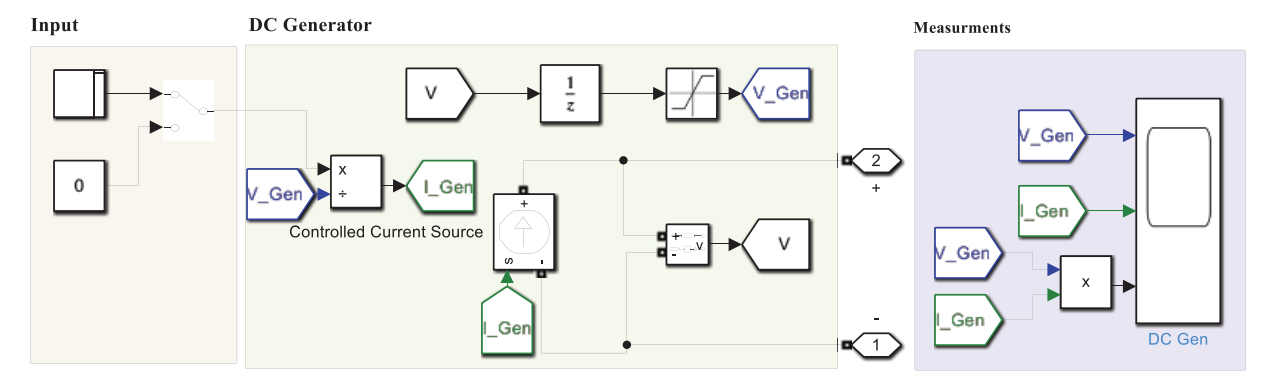


Fig. 6. Modeling of DC diesel generator system configuration.

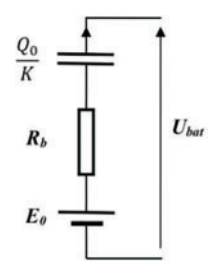


Fig. 7. Electrical model of the battery (22).

resistance of the battery (Ω) , I_b is the current flowing through the battery (A), $\frac{\int I_b dt}{Q_0}$ represents the battery's discharge status, Q_0 is the battery's capacity (Ah), U_{bat} is the output voltage of the battery (V).

This paper proposes a lead-acid battery for energy storage, consisting of four strings of four series-connected 12 V batteries (170 Ah each) depicted in Fig. 8. The total capacity provides backup during low wind or solar generation periods. The battery operates in charging mode when the current is positive and in discharging mode when the current is negative. The initial state of charge (SOC) is set at 50%, balancing energy supply and storage. This configuration optimizes cost and reliability for off-grid applications, with a 50% depth of discharge to extend battery life.

2.5. Inverter

To convert DC voltage into AC, a full-bridge inverter is used, as shown in Fig. 9. This system generates four pulse signals that control the IGBT and diode switches, enabling the DC to AC conversion. By modulating the gate signals of the IGBT switches, the inverter ensures the correct switching operations. This setup allows for a smooth AC output with controlled voltage and frequency, making it highly efficient for the proposed HES.

2.6. Step up Transformer

In this paper, a 10 kVA step-up transformer is utilized to increase AC voltage, making it suitable for the 120 V load. This process involves converting electrical energy to magnetic energy and back, utilizing the transformer core to achieve the desired voltage increase. This transformation is essential to ensure that the voltage levels are appropriate for the intended application. Table IV outlines the specifications of the transformer, which is connected to the output side of the inverter:

2.7. Load

Based on the calculations done [1] to supply fresh water for 45 people in McCallum, two single-phase asynchronous machines are considered as presented in Fig. 10, one with a power rating of 0.5 hp for the submersible pump (Inductive Load 1) to extract water from a 16.8 m well, and another with a power rating of 0.75 hp for the RO system (Inductive Load 2). Single-phase asynchronous motors are commonly used in low-power applications such as submersible pumps and small RO systems due to their simplicity, robustness, and cost-effectiveness. Furthermore, in off-grid energy systems, induction motors are preferred due to their efficiency and reliability in starting and running with varying power quality, which is important for areas with renewable energy systems like solar and wind. Additionally, a 0.3 kW resistive load is included to account for the lighting requirements of the plant. The system operation is aligned with the standard voltage, 120 V RMS, and frequency, 60 Hz, specifications in Canada.

3. SIMULATION RESULTS

Six scenarios were considered for the dynamic simulation of a hybrid energy system powering a water treatment facility in McCallum, Newfoundland and Labrador. The system operates continuously (24/7) to provide the community with a water supply and to prevent water from freezing in the pipelines, as average temperatures remain below 0°C for four months of the year. To analyze the variability of the renewable energy sources—solar and wind—specific conditions were applied in each scenario. For the solar energy system, a constant temperature under standard test conditions (STC) was assumed, as temperature has a minor impact compared to irradiance. The wind turbine was modeled with a fixed pitch angle of zero degree. Table V shows each scenario.

- Scenario 1: At time 1, with irradiance at 1000 W/m² and wind speed of 12 m/s, the system runs solely on renewable energy, and the diesel generator remains off.
- Scenario 2: At time 2, irradiance drops to 200 W/m², and wind speed decreases to 6 m/s,

Battery Measurments Bat <Voltage (V) Bat <Current (A): Bat SOC Bat Battery

Fig. 8. Model of the battery system.

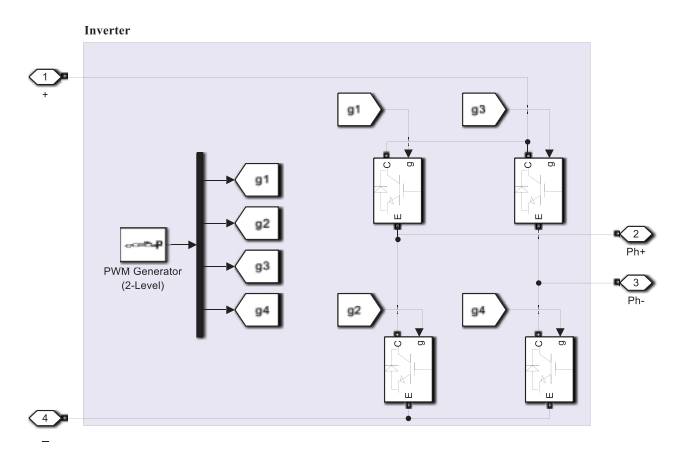


Fig. 9. Inverter system modeled in Simulink.

but the generator is still off, testing the ability of the renewable sources and battery system to meet demand.

- Scenario 3: At time 3, irradiance remains at 200 W/m², but wind speed increases to 10 m/s, and the generator stays off, assessing how increased wind compensates for lower solar output.
- Scenario 4: At time 4, irradiance improves to 800 W/m², but wind speed stays at 6 m/s. The generator remains off, focusing on solar contribution.
- Scenario 5: At time 5, with irradiance at 800 W/m² and wind speed still at 6 m/s, the generator is turned on, testing how the system behaves when backup power is introduced.

• Scenario 6: At time 6, irradiance drops again to 200 W/m², and wind speed is at 10 m/s. The generator is on, ensuring backup power compensates for the reduced solar output.

In our PV system output, the voltage remains constant due to the constant temperature as represented in Fig. 11a. The PV current, shown in Fig. 11b, fluctuates with changes in irradiance. In the first second, when irradiance is at its maximum, the PV current is at its peak, around 50 A, and the PV power, as shown in Fig 11c, reaches approximately 3600 W. At the 2nd and 3rd second, when the irradiance drops to 200 W/m², the PV current sharply decreases to about 10 A, and the PV power proportionally declines to below 1000 W. From the 4th to the 5th second, as irradiance increases again, the PV current rises back to around 40 A, and the PV power increases to around 3000 W. After the 6th second, the irradiance decreases, leading to a corresponding reduction in PV power output.

The dynamic performance of the wind turbine rectifier system is depicted in Fig. 12. Despite fluctuating wind speeds, the rectified voltage remains constant at approximately 48 V. The current and power, however, vary in response to changes in wind speed. At maximum wind speed (12 m/s), the system produces a peak power of 1560 W, which is lower than the nominal 2 kW rating of the wind turbine. This reduction in power output can be attributed to the inherent limitations of wind turbine efficiency, system losses, and suboptimal wind conditions. A short delay is observed between changes in wind speed and the corresponding adjustments in current and power,

TABLE IV: TRANSFORMER PARAMETERS

Parameter	Description	Value	
Nominal power	P_n (VA)	10000	
Nominal frequency	f_n (Hz)	60	
Parameters of primary winding	V_1 (V_{rms}) R_1 (pu) L_1 (pu)	[48/sqrt (2) 0.002 0.08]	
Parameters of secondary winding	V_2 (V_{rms}) R_2 (pu) L_2 (pu)	[120 0.002 0.08]	
Saturation characteristic	i1 phi1; i2 phi2;] (pu)	[0,0; 0.0024,1.2; 1.0,1.52]	
Core loss resistance	[Rm] (pu)	[500]	

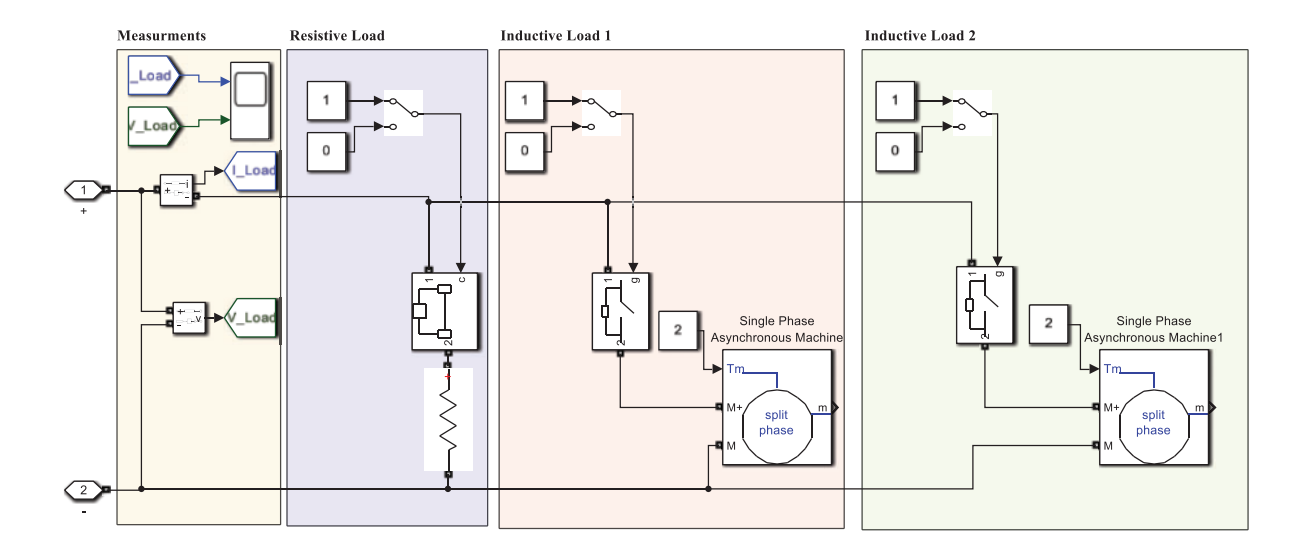


Fig. 10. Load configuration in Simulink.

TABLE V: DETAILS OF EACH SCENARIO

Scenario	Time	Irradiance (W/m ²)	Wind speed (m/s)	Generator relay
1	0	1000	12	off
2	1	200	6	off
3	2	200	10	off
4	3	800	6	off
5	4	800	6	on
6	5	200	10	on

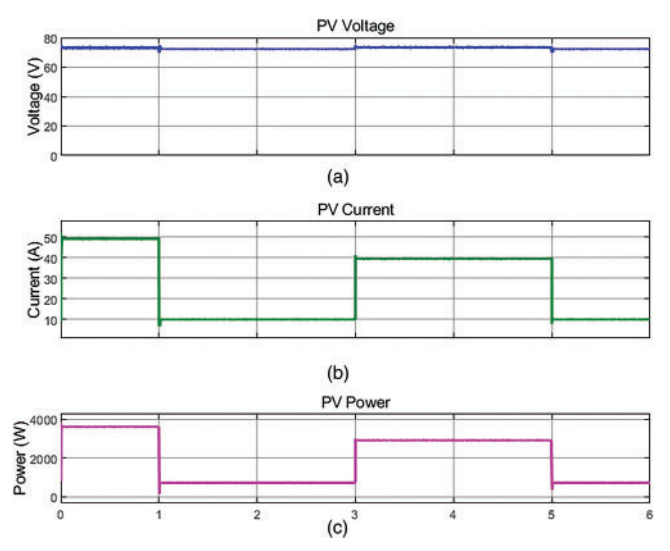


Fig. 11. Dynamic response of PV system: (a) Voltage; (b) Current; (c) Power.

which is caused by the mechanical inertia of the turbine and the response time of the electrical components. Notably, at wind speeds of 6 m/s, the wind turbine produces no power, as this speed falls below the cut-in speed required to generate sufficient torque for power production.

Fig. 13 shows the performance of the DC diesel generator, which activates in the final two seconds when solar and wind sources are insufficient. The DC bus voltage remains steady at 48 V, while the generator current rises to 62.5 A,

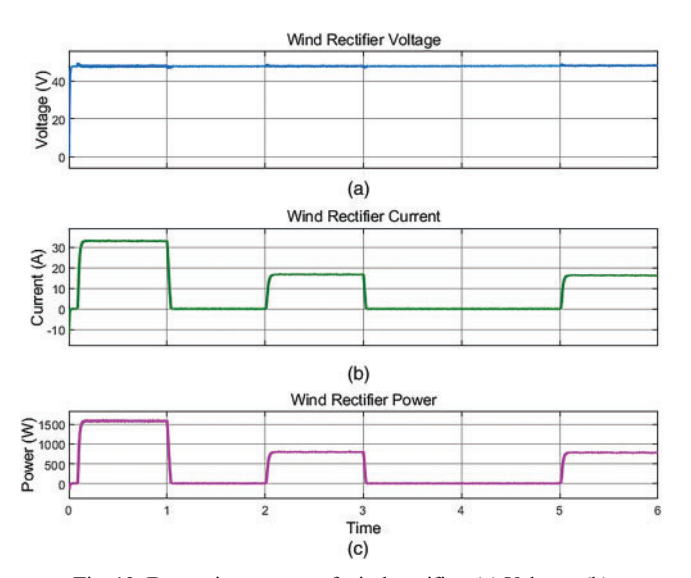


Fig. 12. Dynamic response of wind rectifier: (a) Voltage; (b) Current; (c) Power.

producing 3 kW of power. This demonstrates the generator's role as a reliable backup, ensuring continuous power supply during periods of low renewable energy availability.

Fig. 14 shows the behavior of the battery system, operating at a constant 48 V, as seen in Fig. 14a. From zero to one second, with abundant renewable energy, the battery is charging, indicated by the negative current in Fig. 14b and negative power in Fig. 14c. Between one and two seconds, when renewable energy is minimal and the generator is off, the battery discharges to meet the load, reflected by the positive current and similarly positive power. From two to three seconds, renewable energy is sufficient to supply the load, so there is no need for battery backup, and the battery current drops to zero. Although the generator remains off from three to four seconds, the renewable energy production exceeds the demand, like the first second, causing the battery to switch back to charging mode. After 5th second, the generator is turned on, so the current becomes negative, showing that the battery is no longer needed and is charging again. The state of charge (SOC) remains stable

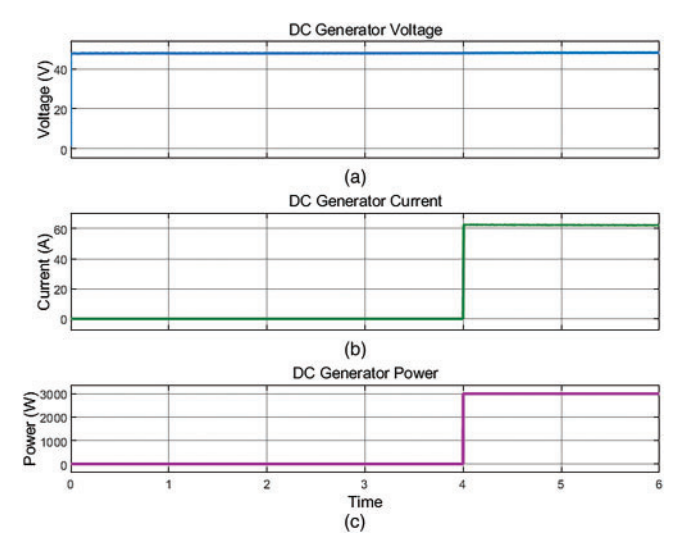


Fig. 13. Dynamic response of DC diesel generator: (a) Voltage; (b) Current; (c) Power.

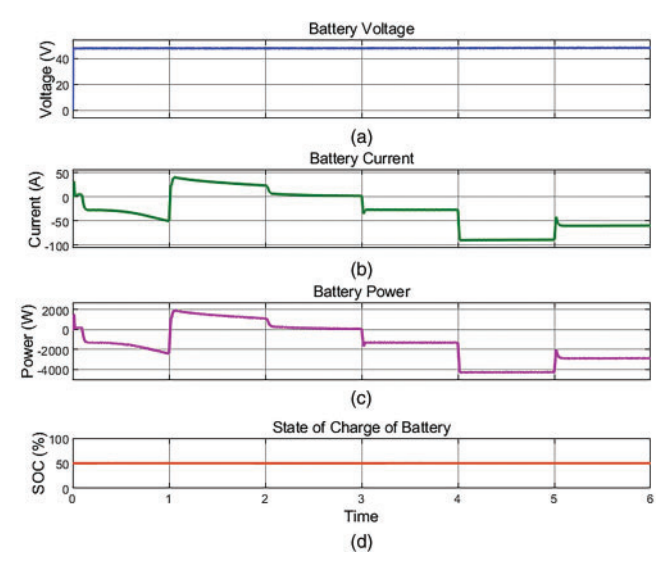


Fig. 14. Battery system performance: (a) Voltage; (b) Current; (c) Power; (d) SOC.

throughout the simulation, as seen in Fig. 14d, ensuring efficient charge cycles and long-term battery health.

Fig. 15a shows the current through the load. At the start of the simulation, the current is a bit higher, which is due to the inrush current that occurs when connecting our load which is mostly inductive. After that, the current gradually stabilizes, and the fluctuations decrease as the system reaches a normal operating state. The sinusoidal nature of the current is expected and the reduction in amplitude over time suggests that the initial demand was met, allowing the system to settle into a steady rhythm.

In Fig. 15b, the voltage across the load was held steady at around 120 V RMS throughout the entire simulation, which means the system is delivering the required voltage without any issue.

4. Conclusion

To supply fresh water to the remote community of McCallum in Newfoundland and Labrador, a continuous water system was designed. To optimize costs and enhance

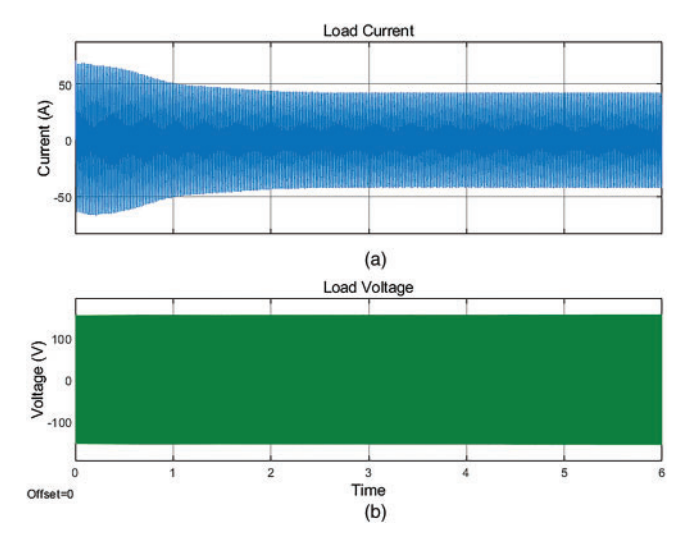


Fig. 15. Load response under continuous operation (60 Hz, 120 V RMS): (a) Voltage, (b) Current.

reliability, an HES was proposed, including a PV system, wind turbine, and, for backup, a small DC diesel generator and battery. The dynamic analysis of the system was performed using MATLAB/Simulink, and it was observed that the two renewable sources operated effectively under varying weather conditions. It was also confirmed that in cases of reduced renewable energy availability, the battery system and diesel generator can reliably support the load, while maintaining a stable output with a pure sine wave at a frequency of 60 Hz. Additionally, the battery management system ensures efficient charge/discharge cycles, preventing overuse and extending the system's lifespan. This combination of renewable energy sources and backup systems ensures both economic efficiency and operational reliability for continuous water supply at selected site.

ACKNOWLEDGMENT

The authors would like to thank their institution for the financial support of this article.

CONFLICT OF INTEREST

The authors declare that they do not have any conflict of interest.

REFERENCES

- Kafrashi Fatemeh, Iqbal Tariq. Sizing optimization and economic modeling of a stand-alone hybrid power system for supplying RO system in McCallum. Journal of Electronics and Electrical Engineering. 2024;3:340-61. ISSN 2972-3280.
- Xevgenos D, Moustakas K, Malamis D, Loizidou M. An overview on desalination & sustainability: renewable energy-driven desalination and brine management. Desalination and Water Treatment. 2014;57(5):2304-14. doi: 10.1080/19443994.2014.984927.
- Jose D, Jeyaprabha SB. Design and simulation of wind turbine system to power RO desalination plant. International Journal of Recent Technology and Engineering. 2013;2(1):102-5
- Syed IM. Near-optimal standalone hybrid PV/WE system 2017;157:727-34. Solar sizing method. Energy. 10.1016/j.solener.2017.08.085.
- [5] Cervantes-Rendón E, Ibarra-Bahena J, Cervera-Gómez LE, Romero RJ, Cerezo J, Rodríguez-Martínez A, Dehesa-Carrasco U. Rural application of a low-pressure reverse osmosis

- desalination system powered by solar-photovoltaic energy for Mexican Arid Zones. Sustainability. 2022;14(17):10958. 10.3390/su141710958
- Apolinário R, Castro R. Solar-powered desalination as a sustainable long-term solution for the water scarcity problem; case studies in Portugal. Water (Basel). 2024 Jul 29;16(15):2140.
- Loutatidou S, Liosis N, Pohl R, Ouarda TBMJ, Arafat HA. Wind-powered desalination for strategic water storage: Technoeconomic assessment of concept. Desalination. 2017;408:36-51. doi: 10.1016/j.desal.2017.01.002.
- Eltamaly AM, Ali E, Bumazza M, Mulyono S, Yasin M. Optimal design of hybrid renewable energy system for a reverse osmosis desalination system in Arar, Saudi Arabia. Arab J Sci Eng. 2021;46:9879-97. doi: 10.1007/s13369-021-05645-0.
- Oladeji AS, Akorede MF, Aliyu S, Mohammed AA, Salami AW. Simulation-based optimization of hybrid renewable energy system for off-grid rural electrification. Int J Renew Energy Develop. 2021;10(4):751–64. doi: 10.14710/ijred.2021.34912
- Canada Natural Resources. Solar resource, NSRDB PSM global horizontal irradiance (GHI)-North American cooperation on energy information. Open Government Portal. 2021. Available from: https://open.canada.ca/data/en/dataset/a2dd0554-03f8-4edc-a3b3-67b47c5c9d6d/resource/30e3825d-adc3-428a-804a-46ff58f71da3.
- [11] Panasonic Solar Panel (Module), 300 Wp, 72-cell, Black on Black-Arntjen Clean Energy Solutions [Internet]. [cited 2024 Nov 5]. Available from: https://store.arntjencleanenergy.com/prod ucts/panasonic-solar-panel-module-300w-72-cell-black-on-black?p r_prod_strat=e5_desc&pr_rec_id=c27738c3b&pr_rec_pid=685436 1841815&pr_ref_pid=5510759645335&pr_seq=uniform.
- [12] Raziya F, Afnaz M, Jesudason S, Ranaweera I, Walpita H. MPPT technique based on perturb and observe method for PV systems under partial shading conditions. MERCon 2019-Proceedings, 5th International Multidisciplinary Moratuwa Engineering Research
- [13] Dileep G, Singh SN. Maximum power point tracking of solar photovoltaic system using modified perturbation and observation method. Renewable and Sustainable Energy Reviews. 2015;50:109-29. doi: 10.1016/j.rser.2015.05.013.
- [14] Environment and Climate Change Canada. (n.d.). Historical climate data. Government of Canada, Retrieved November 7, 2024, from. Available from: https://climate.weather.gc.ca/historical_data/ earch historic data e.html.
- [15] Chong CH, Rigit ARH, Ali I. Wind turbine modelling and simulation using Matlab/SIMULINK. IOP Conf Ser. Mat Sci Eng. 2021;1101(1):012034. doi: 10.1088/1757-899X/1101/1/012034.
- Singh N. Bhupal S. (n.d.). Simulink-based modeling, design, and performance evaluation of PMSG-based wind energy conversion system. J Multi-Dis Eng Technol (JMDET). ISSN: 0974–1771.
- [17] Babu BC, Mohanty KB. Doubly-fed induction generator for variable speed wind energy conversion systems: Modeling & simulation. Int J Comp Electri Eng. 2010;2(1):141-7. doi: 10.7763/IJCEE.2010.V2.141.
- [18] Innotec Power. (n.d.) Innotec Power. 2 kW 48 Volt BLDC Motor. Retrieved August 18, 2024, from. Available from: https://www. pmgenerators.com/home/brushless-dc-motors/48-volt-motors/255ne48-075-2kw-pmsm/
- [19] Jeong HG, Seung RH, Lee KB. An improved maximum power point tracking method for wind power systems. *Energies*. 2012;5(5):1339–54. doi: 10.3390/en5051339.
- [20] Sarkar J, Khule SS. A study of MPPT schemes in PMSG based wind turbine system. International Conference on Electrical, Electronics, and Optimization Techniques, ICEEOT 2016, 2016.
- [21] Bouchebbat R, Gherbi S. A novel optimal control and management strategy of stand-alone hybrid PV/wind/diesel power system. J Control, Automat Electri Sys. 2017;28(2):284-96. doi: 10.1007/s40313-016-0290-y.
- [22] Tahiri FE, Chikh K, Khafallah M. Optimal management energy system and control strategies for isolated hybrid solar-windbattery-diesel power system. Emerg Sci J. 2021;5(2):149-62. doi: 10.28991/esj-2021-01264.